IAC–20–A6,6,7,x58014

Momentum Based Classification for Robotic Active Debris Removal

Shubham Vyas
DFKI-RIC, Germany, Shubham.Vyas@dfki.de

Marko Jankovic
DFKI-RIC, Germany, Marko.Jankovic@dfki.de

Frank Kirchner
DFKI-RIC, Germany, Frank.Kirchner@dfki.de

Recent spacecraft collisions with debris and various near misses have highlighted the need for pursuing Active Debris Removal (ADR) of space debris. Robotic manipulators provide a versatile way to capture, detumble, and eventually deorbit the debris. This paper explores the classification of space debris and robotic manipulators based on angular momentum. Previous classifications have considered the tumble rates, size, and orbit of the debris. However, a momentum-based classification gives an additional insight into the method selection for debris removal as shown in this paper. A study on the momentum capture capabilities of previously flown robotic manipulators is performed. This gives an impression of the capabilities of the flight-heritage robotic manipulators for their use in ADR missions. Furthermore, an analysis is also performed on the momentum of cylindrical space debris as it closely represents the spent rocket upper stages which could be prime targets for a robotic ADR mission. The change in momentum due to the tumble rate and inertia is analysed for such cylindrical debris and they are then categorized based on their momentum. These analyses provide the data required to perform a matching of the momentum of the debris with the momentum capabilities of the existing robotic manipulators and thus classify the debris based on momentum. The classification is then applied to real debris objects and the results are discussed. The comparison of the momentum of debris and manipulators is also used to provide input for future manipulator development for ADR missions.

Acronyms

ADR Active Debris Removal

ESA European Space Agency

ETS-VII Engineering Test Satellite No. 7

LEO Low Earth Orbit

OOS On-Orbit Servicing

SRMS Shuttle Remote Manipulator System

SSRMS Space Station Remote Manipulator System

TRACER the onTology foR ACtive dEbris Removal

URDF Unified Robot Description Format

Vespa Vega Secondary Payload Adapter

I. Introduction

It is well acknowledged that space debris is currently an ever-increasing problem, especially in the Low Earth Orbit (LEO) region [1]. In [2], it can be seen that a significantly large share of the debris objects in terms of number as well as mass are the rocket bodies used to launch the satellites. These are, for the most part, the upper stages of the rockets used for the final burn before satellite deployment and were historically (and still commonly) left in space after satellite deployment. Guidelines for space debris mitigation require the *passivisation* of the rocket upper bodies i.e. all on-board stored sources of energy must be released and emptied [3]. However, this guideline was first published in 1997 [4] and the rocket upper stages before that were not necessarily passivated. Even though passivisation is now common, upper stage break-ups still occur such as those reported in the following references:[5], [6], [7]. Notwithstanding the guidelines that have existed for spacecraft and rocket bodies for reducing space debris, it can be seen that the number has been increasing at a significant rate

in the last decade [1], [2], [8].

Due to this, ADR has been suggested as a method of reducing debris such that the orbits do not become unusable [9]. However, considering the variety of space debris, their orbital regimes and currently studied ADR methods, choosing one over the other, even if for a specific target object, is a challenging task due to the dimensions of the parameter space characterizing the problem at hand [10]. Furthermore, the available data about the space debris and the studied ADR methods is often incoherent and unstructured which points to a more fundamental problem currently afflicting the ADR domain, the *information paradox* [11], [12]. To obviate this situation in recent years several knowledge organization systems (such as taxonomies, ontologies and knowledge graphs) were developed [10], [12]–[19]. These methods are capable not only of systematically storing and categorizing data, but also allowing inference of new knowledge, that would otherwise be obscured by the shear amount of available data. However, out of the mentioned studies only [10], [12] focus on the ADR domain, or more specifically on the domain of ADR capture methods, with an aim to define a standardized, machine-interpretable vocabulary of characteristics of objects that allows for an automatic inference of most suited ADR capture methods, safety wise. This way the initial mission planning can be made easier by allowing ADR researchers to analyze quickly the domain of interest and infer new knowledge, while at the same time keeping the parameter space of each object hidden from the user, reducing the complexity and possibility of a human error [12]. Nevertheless, the onTology foR ACtive dEbris Removal (TRACER) developed within [12] does not, in its current iteration, consider axioms related to the shape of an object nor its mass characteristics which might be problematic in case of specific ADR capture methods, such as the robotic manipulator. In fact, in the context of ADR, manipulator-based systems are mainly associated with targets having stable to medium tumbling attitude regimes [12]. However, it can be seen that even slow tumble rates ($\approx 5\,^\circ\,\mathrm{s}^{-1}$) can lead to very-high joint torques on the robot arms used for capture if the momentum of the debris is not considered [20]. This is because a slow-rotating object can have a high angular momentum/kinetic energy (due to high inertia) which has to be dissipated during the ADR operation for post-capture stabilization.

To bridge this gap, in this paper, we propose an additional quantity based on which a classification can be carried out: the target's *angular momentum*. This can be used in conjunction with the current classification methods for improved matching of the debris objects with the removal methods. For this, we consider the case of ADR using a robotic manipulator which has to absorb the angular momentum of the target for post-capture stabilization. We consider previously space-flown robot arms and classify an artificial dataset along with sparse real data which has been pre-classified using state of the art ontology-based method (TRACER) described in [12].

The layout of this paper is as follows: section 2 describes the methodology of the classification along with the relevant momentum calculations of the debris and robot manipulation given in subsection 2.1 and subsection 2.2 respectively. In section 3, the *Momentum-Based Classification* is carried out with subsection 3.1 showing the classification of generated dataset and subsection 3.2 demonstrating the classification on real debris data pre-classified using an ontology-based method. A discussion based on the classification results is carried out in section 4 followed by conclusions and future work given in section 5.

II. Methodology

The methodology followed in this paper is as follows: initially, an artificial dataset for cylindrical space debris with varying mass, inertia (size), and rotation rates is generated. From this, a sample dataset is considered for classification and visualization. Then, the technique for computing the momentum capture capability for robot arms with a free-floating base is provided along with its application to 3 space-flown manipulators. This data is then used to classify the dataset generated earlier based on the angular momentum computed in both sections. Furthermore, a sparse dataset which is pre-classified using state of the art ontology-based method for ADR method selection is classified based on the computed angular momentum of the debris. This is followed by a discussion on the ramifications on including angular momentum in the classification of space debris based on the results obtained in this paper.

This leads to the classification of debris, specifically rocket upper stages, based on the momentum capabilities of the robot arms described in section 2. This is referred to as *Momentum Based Classification*: the classification of space debris based on their angular momentum and the current angular momentum capabilities of the space-qualified robot arms.

II.i Space Debris Momentum Data Generation

Even though a lot of data is available about space debris, specifically, their size and their orbits [21], it is extremely sparse to find any data on their rotation rates. This is because the data gathered for space debris is done using ground-based telescopes and extracting rotation information from ground-based telescopes is extremely challenging using the current technology [22]–[25].

Due to this, an artificial dataset of momentum values for various space debris was generated for this paper. The focus was aimed at the upper stages of various rockets used to launch satellites. After the release of the satellite, these upper stages tend to stay in orbit for a long time. Generally, these are passivated to release the stored energy and prevent any future explosion leading to fragmentation and unwanted debris generation [3]. After passivation, the upper stages tend to stay in orbit. The number of upper stages can seem low when compared to the number of fragmentation debris objects but they form the highest mass fraction of non-operational objects in space i.e. debris [2]. This makes them a prime target for removal as removing them amounts to removing a major mass of debris which can prevent future fragmentation events due to collisions/breakups. Due to these considerations, rocket upper stages have been of high interest and recently European Space Agency (ESA) awarded a contract to remove a piece of debris from the VEGA upper stage: Vega Secondary Payload Adapter (Vespa) [26].

To generate the momentum data for cylindrical objects representing used rocket upper stages, the dimensions of the various upper stages from different rockets were taken into account. These include the Centaur upper stage from the Atlas V rocket [27], Ariane 5 Second stage [28], Falcon 9 Second Stage [29], Soyuz Volga and Fregat Upper Stages [30] [31], Vega AVUM Upper Stage [32], and the Delta Cryogenic Second Stage [33]. In Table 1, the dimensions and masses of these upper stages are given. The mass and dimensions of the space debris objects were varied and their momentum was calculated for different spin rates about their *X, Y,* and *Z Axis*. This gives an extensive database of various debris and their momentum at various tumbling rates.

From each of these upper stages, the upper and lower limits for the length and the diameter of the cylinder was determined. For the mass, the lowest dry mass was taken as the lower limit and the upper limit was taken from the maximum dry mass upper stage along with a 10% margin for leftover propellant as an extremely conservative estimate. For the sake of simplicity, the sloshing effect of the propellant was not considered in this study. The inner radius of the cylinder is taken as 90% of the outer radius, thus the mass of the cylinder is assumed to be the concentrated at the outer 10% volume of the shell. The parameters used to generate the full momentum dataset for cylindrical objects can be seen in Table 2.

From this dataset, a sample can be considered for the sake of visualization and demonstration of the momentum-based classification method. For this sample data, we consider the change in momentum with the change in mass and rotation velocities about the Z axis while keeping all other parameters constant The numbers given below are thus only given for the purpose of illustration.The upper stage's mass is varied between 1000 kg to 3000 kg as it covers most of the upper stages given in Table 1. The rotational velocities about the Z axis vary between $1\,^\circ\,s^{-1}$ to $20\,^\circ\,s^{-1}$. The height, outer diameter, and the rotational velocities about the X and Y axis are kept constant at 4.25 m, 3.75 m, and $1\,^\circ\,s^{-1}$ for both axes respectively. This sample data can be seen in Figure 1 where the change in the angular momentum with the change in the mass and the angular velocity about the Z-axis of rotation is represented by the size of the circle at the given data point. It shows the increase in angular momentum as both mass and rotation rate changes.

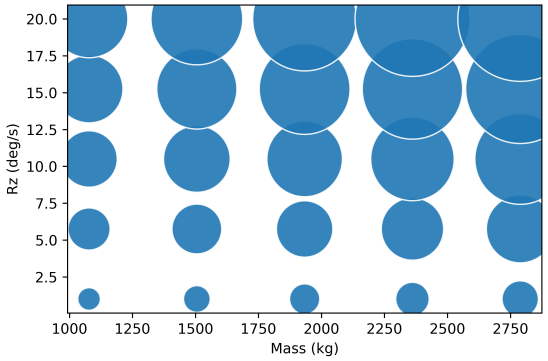

Fig. 1: Change of Momentum with Mass and Z-Rotation Velocity

II.ii Robot Arms Momentum Data Generation

To classify and assess if a robot arm can capture specific space debris, the angular momentum capabilities of robotic manipulators are computed. For this, the robot arms considered were those that have al-

Table 1: Upper Stages of Various Rockets

Rocket Upper Stage	Height (m)	Diameter (m)	Min. Mass (kg)	Max Mass (kg)
Soyuz Fregat Upper Stage [30]	1.5	3.35	902	7540
Arianne 5 ESC-A [28]	4.711	5.4	4540	19440
Atlas V Centaur [27]	12.68	3.05	2528	23288
Delta Cryogenic Upper Stage [33]	13.7	5.1	3840	30700
Falcon Heavy 2nd Stage [29]	NA	3.66	NA	NA
Soyuz Volga Upper Stage [31]	1.025	3.2	840	1740
Vega Upper Stage AVUM [32]	2.04	2.18	688	1265

Table 2: Parameters for Cylinder Momentum Dataset

Parameter	*Min*	*Max*	*Data Points*
Mass (kg)	650	4500	10
Height (m)	1	14	5
Outer Diameter (m)	2	5.5	5
Rotation X-Axis (deg/s)	1	20	5
Rotation Y-Axis (deg/s)	1	20	5
Rotation Z-Axis (deg/s)	1	20	5

ready been flown to space. The motivation for this is as follows: if the robotic manipulator has previously flown to space, then it has already been through the process for flight qualification. And due to this, all the components of the manipulator are flight qualified. This allows the results from this study to be used to create a new robot arm (or use an existing design) from the pre-flight qualified components such that the time-to-flight is reduced.

The models of the robot arms were created in the Unified Robot Description Format (URDF), which is an XML format for representing a robot model. Since not many URDF models exist for the pre-flown robot arms, information from available published literature was used to create the models. The following robot manipulator models with complete kinematic and dynamic parameters were created:

- Engineering Test Satellite No. 7 (ETS-VII) Spacecraft and Robot Arm from [34] and [35].
- Shuttle Remote Manipulator System (SRMS) i.e. Canadarm from [36].
- Space Station Remote Manipulator System (SSRMS) i.e. Canadarm2 from [36].

To avoid the repetition of this task in the future by other robotics researchers, these models were published as initial models in an open-source GitHub repository: Traceable Robot Models [37]. This repository will be used in the future to add more robot models from literature as they are developed.

For momentum based classification, the momentum capabilities of the manipulator arms are evaluated from the models. For this, a global search in the manipulator state space, consisting of the joint position and velocity space, can be performed. However, such a search, while giving the maximum momentum the robot arm can exert, does not provide insights into the momentum capture capability in relation to the debris capture problem. It can be easily seen and verified in simulation (using Equation 1) that a robot arm will exert the maximum momentum if it starts in a fully extended position and all main-axis joints rotate with maximum velocity so that all the links of the arm move in the same direction. Such momentum capability, while calculable, does not provide any insight. Hence, it was decided to use a capture configuration for a robot arm as the initial configuration and the momentum search is carried out in the neighbourhood of this configuration. This raises the following question: *Which configurations of the robot arm qualify as capture configurations?* To answer this, the following requirements were devised, which when met, a configuration can be called as one of the capture configurations:

- The position of joints should not be close to the joint limits, if any.
- The end-effector should be facing away from the base-satellite towards a hypothetical target for capture.
- The end-effector position should not be nearby to the base of the manipulator arm.
- The configuration should not be close to a kine-

matic singularity i.e. have high kinematic manipulability.

- The configuration should not be close to a dynamic singularity i.e. have high dynamic manipulability.

Configurations that comply with all the mentioned requirements were found for each of the arms. For each arm, the kinematic and dynamic manipulability at the initial capture configuration was verified to be high so that the arm is not close to a singular configuration. From here on, the neighbourhood of the capture configuration can be defined using the maximum allowed joint deviations from the configuration. For this, a maximum joint deviation of 10° was used. This gives the manipulator freedom to move without violating any of the singularity constraints and avoid self-collisions or collisions with the base. Along with this, the maximum specified joint velocity was varied from 2 °/s to 20 °/s. The joint rate limit for the SSRMS/Canadarm is $4\,^\circ\,\mathrm{s}^{-1}$ for an unloaded arm [36]. The reason for choosing a higher range of joint rates is to have a more future-facing view and this is further discussed in section 4.

Once the neighbourhood of state space (joint positions and velocities) was defined, the linear and angular momentum can be calculated using the following equation from [38]:

$$\begin{bmatrix} P \\ L \end{bmatrix} = H_0 \begin{bmatrix} V_0 \\ \omega_0 \end{bmatrix} + H_{0m}\dot{\phi} \qquad [1]$$

Where,

P = Linear Momentum Vector ($\mathrm{kg\,m\,s^{-1}}$)
L = Angular Momentum Vector ($\mathrm{kg\,m^2\,s^{-1}}$)
H_0 = Base Inertia Tensor
V_0 = Base Linear Velocity Vector ($\mathrm{m\,s^{-1}}$)
ω_0 = Base Angular Velocity Vector ($^\circ\,\mathrm{s^{-1}}$)
H_{0m} = Dynamic-Coupling Inertia Matrix
$\dot{\phi}$ = Joint Velocity Vector ($^\circ\,\mathrm{s^{-1}}$)

An implicit assumption made here is that the initial linear momentum of the base is zero [38]. As this work is focused on the angular momentum capabilities of the manipulator, the base spacecraft's angular and linear velocity are assumed to be zero. This satisfies the zero base linear momentum assumption. Furthermore, this also entails that the attitude control system's momentum contribution is not considered as the base is taken to be stationary. Using the above given equation the maximum angular momentum exerted by the robot arm in the neighborhood of the capture configuration is found using an optimisation based approach using the MATLAB function "*fmincon*".

The angular momentum that can be stored/exerted by the robot arms along with the maximum allowed joint velocities can be seen in Figure 2. It can be seen that the angular momentum stored in the arm is directly proportional to the joint velocity limit as expected from Equation 1. Furthermore, the larger arm such as the SSRMS/Canadarm2, which has a higher inertia for its links, have a higher slope for Joint velocity vs Angular Momentum when compared to the small arm such as the ETS-VII arm. The angular momentum capacity of each arm is the maximum angular momentum the arm can exert while allowing for a maximum joint velocity of $20\,^\circ\,\mathrm{s^{-1}}$.

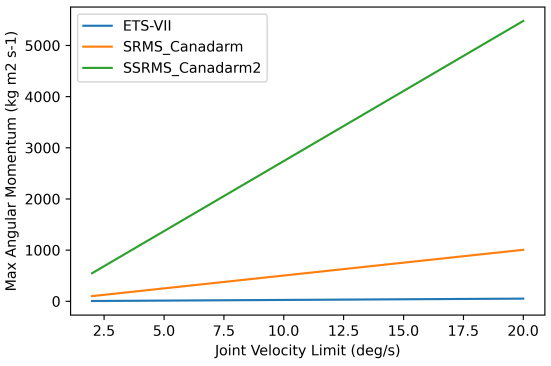

Fig. 2: Momentum Capability of Flown Robot Arms

III. Momentum Based Classification

In this section, we describe and demonstrate a momentum-based classification of space debris. In subsection 3.1, the classification is carried out for the debris dataset generated in subsection 2.1 and the debris is classified based on the robot arm momentum capabilities outlined in subsection 2.2. The classification is then applied to real-world debris objects to explore a more realistic scenario in subsection 3.1.

For the classification carried out in this section, the selection of debris for detumbling was based on the *Bias-Momentum Approach* given in [39] and [40]. This approach was chosen as it aims to minimize the chaser satellite's attitude deviation during the approach of the robot arm to the target and post-capture without utilizing any fuel. This is only possible if the target momentum can be absorbed by the

robot arm and the reaction wheels independently. It does this by pre-loading the robot arm and the reaction wheels of the base spacecraft with angular momentum which is same in value to the debris angular momentum but opposite in direction. This allows the target and the arm to have a net-zero angular momentum after the capture. A rotation-free and zero-fuel usage makes Bias-Momentum detumble the preferred method for *Momentum Based Classification*.

The Bias-Momentum approach includes with it certain assumptions that confine its applicability to a bounded number of ADR situations. Thus, this classification method is applicable when the following assumptions are met (from [39] [40]) for the Bias-Momentum Approach:

- The rotation speed and the inertia properties of the target are known a priori.
- There is no linear motion between the chaser and the target satellite.
- The total momentum of the system is conserved i.e. no external forces and no thruster firings.
- The angular momentum of the target can be stored by the attitude control system of the spacecraft i.e. the reaction wheels.

From the Bias-Momentum Approach described above, it can be seen that for a successful capture without any attitude disturbance of the chaser satellite, the robot arm (and the reaction wheels) should be capable of storing the angular momentum equal to that of the target.

III.i Classification of Generated Data

From the rocket upper stage angular momentum data generated in subsection 2.1, the upper stage debris data from subsection 2.1 can be allocated as following:

- Debris Momentum that can be absorbed by the ETS-VII arm
- Debris Momentum that can be absorbed by SRMS/Canadarm
- Debris Momentum that can be absorbed by SSRMS/Canadarm2

From the given sample debris data in Figure 1, the debris whose momentum can be absorbed by the robot arms can be seen in Figure 3.

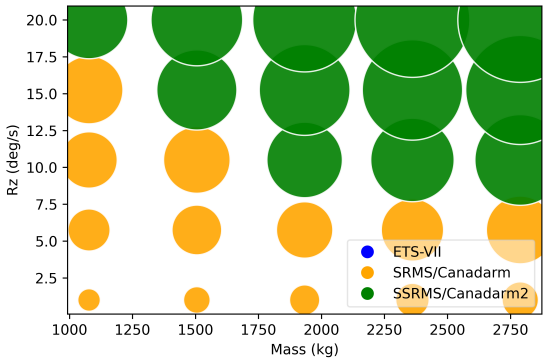

Fig. 3: Sample Data Momentum that can be Absorbed by the Robot Arms.

It can be seen from this figure that the SSRMS/Canadarm2 robot manipulator has a theoretical capability to capture the momentum of all the debris objects in the sample dataset. Along with this, the SRMS/Canadarm is also able to capture cylindrical rocket upper stages rotating at $\approx 10\,^{\circ}\,\mathrm{s}^{-1}$ up to a mass of 1500 kg. The ETS-VII robot arm does not have the capability to capture any debris in this sample data. As seen from Figure 3, momentum-based classification can be useful in finding debris objects which can be captured using the currently available robotic technology.

A more practical classification can be carried out using the data from real debris. This is shown in the following section.

III.ii Classification of Real Data

The validity of the developed classification was tested on the real data by applying it on top of the results of TRACER which consists of 210 ontology individuals associated to 30 large intact cataloged objects (19 payloads and 11 rocket bodies) [12]. The reason for building on top of the results of TRACER stems from its ability to identify for each debris object its most suited ADR capture method(s) not only according to its attitude regime, on-board propellant and object type but also according to its breakup criticality as well as its degree of uncooperativeness [12]. This way among the 30 objects processed by TRACER we were able to select, for the purposes of the current paper, only four specific target objects.

The four objects considered for the momentum-based classification have the following international designators: *2009-017B*, an Atlas V 421 Centaur Upper Stage, *1991-084C*, an Ariane 44L H10 upper

stage, *2001-045D*, a Proton Blok-DM-2 upper stage, and *1995-026D*, a Molniya-M Blok-2BL upper stage. Details of the these objects can be found in the ESA's DISCOS [21]. These were selected from the TRACER dataset for the following reasons: the shape of these objects is cylindrical and they do not have solar panels, thus in-line with the work presented in this paper, and their rotation rates are between $1\,^\circ\,s^{-1}$ and $20\,^\circ\,s^{-1}$. Emphasis was placed on the availability of data regarding the weight and dimensions of the debris object. As described previously in subsection 2.1, a scarcity of data exists for the angular rates and masses of the debris. These objects were selected as information about them was readily available from public sources. These debris objects have been classified by TRACER as to be removed using either a net-based method or a manipulator-based method. The angular momentum for these debris is calculated and checked if it can be absorbed by a space-flown robotic manipulator.

The given debris objects and the removal method from [12], along with the computed absolute angular momentum, are given in Table 3.

The angular momentum of these objects is computed assuming the rotation rate to be only about the axis of the cylinder, i.e. the axis of maximum inertia, to find the maximum possible angular momentum of the debris object. This can then be compared with the angular momentum capture capabilities of the robot arms in subsection 2.2. Along with the maximum joint rate of $20\,^\circ\,s^{-1}$ as taken in the previous section, the current joint limit of SSRMS/Canadarm2 of $4\,^\circ\,s^{-1}$ ([36]) is also taken into account while computing the robot arm angular momentum capability. This provides a more realistic view of the capture capabilities using the currently space-qualified joint actuators. The robot arms that were matches with the respective debris, i.e. that could capture the momentum of the debris, can be seen in Table 4.

IV. Discussion

From section 3, it can be seen that debris data, both generated and from real-data sources can be classified based on their angular momentum and the angular momentum of the currently space-flown robot arms, albeit with some innate challenges.

In Figure 3, it can be seen that the SSRMS/Canadarm2 robot manipulator can absorb all, SRMS/Canadarm can absorb about half, and the ETS-VII robot arm can absorb none of the angular momentum of the debris in the sample dataset. This analysis is based solely on the absolute angular momentum of the debris and the arm. It should be noted that the ability to absorb the angular momentum does not imply the capture of the debris itself. One of the reasons for this is that the momentum computations used a joint velocity limits of $20\,^\circ\,s^{-1}$, however, the SSRMS/Canadarm2 is only qualified for operation with max joint velocity of $4\,^\circ\,s^{-1}$ [36]. Furthermore, an object of length 4.25 m and diameter 3.75 m poses extreme difficulties for capture while rotating at $20\,^\circ\,s^{-1}$ about any axis.

The robot arms used in this study were space-qualified and have already been flown to space for successful missions. This is significant as the parts and designs used for these arms are space-qualified and hence can facilitate the design of future manipulators specific for ADR. On the other hand, the joint velocity limits used in subsection 3.1 are not the exemplar of the robot arms flown to space. They are more akin to the robot arms used in the terrestrial industries. The joint velocity limit of $20\,^\circ\,s^{-1}$ is generally on the lower end of the spectrum when looking at robust industrial arms used for manufacturing, welding, etc. The current industrial arms regularly provide over $50\,^\circ\,s^{-1}$ joint velocities with payloads over 1000 kg [41]. Years of research and development invested in the industrial joint actuators has increased their reliability and maturity. These technologies can be transferred to the future manipulators for ADR/On-Orbit Servicing (OOS) missions thus bringing along the high-speed joint velocities.

Barring the high angular rate debris, it is noteworthy to see that the upper stage debris (in the generated dataset) of various sizes and masses could be captured by the given robot arms. In Table 4, a portion of the results of debris classification from TRACER ([12]) are viewed through the lens of *Momentum-Based Classification*. Here, two things can be observed about the ADR methods assigned to the debris: one of the net-based capture target's angular momentum can be absorbed by a robot arm with current joint velocity limits, and the angular momentum of one of the debris which is assigned for robot arm-based removal method cannot be absorbed with any currently available space-flown robot arm. However, even though the robot arm could absorb the momentum of the debris that have been selected for the net-based capture, it is not necessarily the preferred choice as the pre-classification considers factors such as *Grapple feature existence, Capture interface material, and Capture interface clearance* (from [12]). For the debris whose angular momentum cannot be absorbed by any currently available robot arm, the

Table 3: Space Debris Object's Properties

COSPAR ID	Name	Mass (kg)	Length (m)	Diameter (m)	Rotation Rate ($^\circ\,s^{-1}$)	Removal Method	Angular Momentum ($kg\,m^2\,s^{-1}$)
2009-017B	Centaur-5 SEC (Atlas V 421)	2020	11.7	3.1	6.35	net	1947
1991-084C	H10 (Ariane 44L H10)	1764	11.42	2.6	1.735	net	327.73
2001-045D	Blok-DM-2 (Proton-K/DM-2)	2440	6.3	3.7	4.65	net/robot arm	2453.4
1995-026D	Blok-2BL (Molniya-M Blok-2BL)	892	2.3	2.2	9.95	net/robot arm	678.51

Table 4: Debris and Robot arm Matching

COSPAR ID	Angular Momentum ($kg\,m^2\,s^{-1}$)	Removal Method	Matched Robot Arms ($20\,^\circ\,s^{-1}$)	Matched Robot Arms ($4\,^\circ\,s^{-1}$)
2009-017B	1947	net	SSRMS	-
1991-084C	327.73	net	SRMS/SSRMS	SSRMS
2001-045D	2453.4	net/robot arm	SSRMS	-
1995-026D	678.51	net/robot arm	SRMS/SSRMS	SSRMS

high angular momentum could cause predicaments such as high joint torques during robotic ADR due to its high angular momentum [20]. Thus, this debris object is not suitable for the robotic arm removal method excluding a preceding attitude syncing maneuver. This indicates that momentum data can play a role in the selection of removal method as it provides more information than just the rotation rate that is currently used. Furthermore, all of the debris object's angular momenta can be absorbed by the robot arms if the joint velocity limits are increased to $20\,^\circ\,s^{-1}$. This shows that further development of the joint actuators in the future will enable better ADR capabilities even if other parameters in the design of the arm are kept constant.

From the above discussion, it can be seen that including the angular momentum data in the current classification methods for space debris removal could provide an valuable information towards a more exhaustive selection of ADR capture methods. However, this is not without its limitations. One of the foremost consideration is that this classification is based on the capture capability using the *bias-momentum approach* and thus, has the same assumptions. Even though it gives insight into the debris removal problem, it does not take into account the use of active momentum dissipating devices such as thrusters which could be used to provide detumbling strategies without storing the angular momentum solely in the manipulator arm/reaction wheels. Such methods use the entire system such as is done in [42]. However, classification based on such methods are not computationally efficient considering the large number of possible trajectories the system could take for each scenario. Additionally, data sources for inertia and angular rate for space debris are scarce. Until now, most of the work on space debris cataloguing has been put into the detection of the debris and its orbit determination. Not much effort has been put in cataloguing the inertia parameters of the debris nor their angular velocities. This can be partially attributed to the technological difficultly in estimating the angular velocity of the debris and only recently the angular rate estimation has become interesting for researchers [22]–[25]. Including momentum data to improve the current debris classification techniques

requires detection, identification, and cataloguing the inertial and angular rate parameters of debris. Having catalogued inertia and momentum data further increases the utility of momentum-based classification presented here. Furthermore, momentum-based classification while providing insights into the debris target selection for robotic ADR, does not provide information about target selection for other ADR methods such as net-based or electromagnetic-based methods. This classification method can be expanded in the future to include other capture methods and then be included in a knowledge-based classification framework for most utility.

V. Conclusion and Future Work

In this paper, we provide a method for *Momentum-Based* classification of space debris that can be used to improve the selection of an ADR capture method. Current classification methods use a variety of parameters for debris classification such as orbital parameters, attitude regime etc. Some of the classification methods also provide a framework for the inference of ADR methods most suited to capture a specific debris object. However, none of the methods consider the target's angular momentum. Momentum-based classification bridges this gap as it accounts for the inertia (and thus shape and mass) and the rotation velocity of the debris while selecting a robotic-based method for ADR. This method for classification constitutes the computation of angular momentum of debris as well as the momentum limits of the considered robotic manipulators. Then the debris capture is defined based on the momentum capture capabilities of the robot arm using the Bias-Momentum capture and detumble method. This classification was carried out on an artificially generated dataset of tumbling cylinders representing upper stage debris and consequently applied to real cylindrical debris objects. From this, we can show that the currently available space-flown robot manipulators have the capability to absorb the angular momentum of various upper stage debris. This capability can be further increased by simply developing joint actuators with higher velocity limits without any changes to the rest of the space-qualified robot arm. As this work was limited to cylindrical objects only, the future work aims to generalize this method of debris classification by applying it to wider types of debris objects which can be captured by a robotic arm such as upper stages or cylindrical satellites with solar panels, and generic satellite shapes such as a box with panels. Furthermore, considering the limited scope of the current implementation of the developed method our future work will consist in implementing it within a knowledge management system, such as TRACER, as an axiom to further improve the current state of the art.

Acknowledgment

This research was conducted within Stardust Reloaded project which has received funding from the European Union's Horizon 2020 research and innovation programme under the Marie Skłodowska-Curie grant agreement No 813644

References

[1] ESA Space Debris Office, "ESA's Annual Space Environment Report," Tech. Rep. July, 2019, pp. 1–78. [Online]. Available: https://bit.ly/2Soiqfi.

[2] P. D. Anz-Meador, "Orbital debris Quarterly News," *NASA*, vol. 24, no. 1, 2020.

[3] U.S.A Government, "U.S. Government Orbital Debris Migration Standard Practices," Tech. Rep., 2009.

[4] NASA, *NASA Orbital Debris Program Office*. [Online]. Available: https://orbitaldebris.jsc.nasa.gov/mitigation/ (visited on 09/14/2020).

[5] V. Agapov, "Major fragmentation of Atlas 5 Centaur upper stage 2014-055B (SSN #40209)," in *IAA Space Debris Committee meeting*, Bremen: IAA, 2018.

[6] L. David, *Cluttering Up Space: U.S. Rocket Stage Explodes*, 2019. [Online]. Available: http://www.leonarddavid.com/cluttering-up-space-u-s-rocket-stage-explodes/.

[7] 18th Space Control Squadron, *Twitter: @18spcs 18th Space Control Squadron*, 2019. [Online]. Available: https://twitter.com/18SPCS/status/1121184362559496192.

[8] P. D. Anz-Meador, "Orbital Debris Quarterly News," *NASA*, vol. 24, no. 2, 2020.

[9] J. C. Liou, "An active debris removal parametric study for LEO environment remediation," *Advances in Space Research*, vol. 47, no. 11, pp. 1865–1876, 2011. DOI: 10.1016/j.asr.2011.02.003.

[10] M. Jankovic and F. Kirchner, "Taxonomy of LEO Space Debris Population for ADR Capture Methods Selection," in *Astrophysics and Space Science Proceedings*, April, vol. 52, 2018, pp. 129–144. DOI: 10.1007/978-3-319-69956-1_8.

[11] L. Orman, *Information Paradox : Drowning in Information, Starving for Knowledge*, en-US, https://bit.ly/2oKFSIe, (accessed 7-July-2019), Jun. 2017.

[12] M. Jankovic, M. Yüksel, M. M. Babr, F. Letizia, and V. Braun, "Space debris ontology for ADR capture methods selection," *Acta Astronautica*, vol. 173, pp. 56–68, Aug. 2020. DOI: 10.1016/j.actaastro.2020.03.047.

[13] M. P. Wilkins, A. Pfeffer, P. W. Schumacher, and M. K. Jah, "Towards an Artificial Space Object Taxonomy," in *Advanced Maui Optical and Space Surveillance Technologies Conference (AMOS)*, vol. 1, Maui, Hawaii, USA: Maui Economic Development Board, Inc., Sep. 2013, pp. 1–18. [Online]. Available: https://bit.ly/2EWSWPH (visited on 01/27/2020).

[14] C. Frueh, M. Jah, E. Valdez, P. Kervin, and T. Kelecy, "Taxonomy and Classification Scheme for Artificial Space Objects," in *Advanced Maui Optical and Space Surveillance Technologies Conference (AMOS)*, vol. 1, Maui, Hawaii, USA: Maui Economic Development Board, Sep. 2013, pp. 1–13. [Online]. Available: https://bit.ly/2ryiH5O.

[15] A. P. Cox, C. K. Nebelecky, R. Rudnicki, W. A. Tagliaferri, J. L. Crassidis, and B. Smith, "The Space Object Ontology," in *2016 19th International Conference on Information Fusion (FUSION)*, Heidelberg, Germany: IEEE, Jul. 2016, pp. 146–153, ISBN: 978-0-9964527-4-8. [Online]. Available: https://bit.ly/360WeNw.

[16] R. J. Rovetto, "An ontological architecture for orbital debris data," *Earth Science Informatics*, vol. 9, no. 1, pp. 67–82, Mar. 6, 2016, ISSN: 1865-0473. DOI: 10/gfxj3m.

[17] R. Furfaro, R. Linares, D. Gaylor, M. Jah, and R. Walls, "Resident Space Object Characterization and Behavior Understanding via Machine Learning and Ontology-based Bayesian Networks," presented at the Advanced Maui Optical and Space Surveillance Technologies Conference (AMOS), Wailea, Maui, Hawaii, USA: Maui Economic Development Board, Inc., Sep. 1, 2016, pp. 1–14. [Online]. Available: https://bit.ly/31kcbeR (visited on 10/17/2019).

[18] B. Liu, L. Yao, and D. Han, "Harnessing ontology and machine learning for RSO classification," *SpringerPlus*, vol. 5, no. 1, Dec. 26, 2016, ISSN: 2193-1801. DOI: 10/gf9zg3.

[19] S. Le May, B. Carter, S. Gehly, and S. Flegel, "Leveraging Web data and graph structures to support rapid space object identification," in *69th International Astronautical Congress (IAC)*, Bremen, Germany: International Astronautical Federation (IAF), 2018, pp. 1–10.

[20] S. Jaekel, R. Lampariello, W. Rackl, M. De Stefano, N. Oumer, A. M. Giordano, O. Porges, M. Pietras, B. Brunner, J. Ratti, Q. Muehlbauer, M. Thiel, S. Estable, R. Biesbroek, and A. Albu-Schaeffer, "Design and operational elements of the robotic subsystem for the e.deorbit debris removal mission," *Frontiers Robotics AI*, vol. 5, no. AUG, pp. 1–20, 2018. DOI: 10.3389/frobt.2018.00100.

[21] ESA Space Debris Office, *DISCOS - Database and Information System Characterising Objects in Space*. [Online]. Available: https://discosweb.esoc.esa.int/ (visited on 08/16/2020).

[22] T. Schildknecht, H. Krag, and T. Flohrer, "Determining, Monitoring and Modelling the Attitude Motion of Potential ADR Targets," in *Proceedings of the Clean Space Industrial Days*, 2016.

[23] T. Schildknecht, J. Silha, J.-N. Pittet, and A. Rachman, "Attitude states of space debris determined from optical light curve observations," in *1st IAA Conference on Space Situational Awareness (ICSSA)*, 2017. DOI: 10.7892/boris.106946.

[24] J. Silha, T. Schildknecht, J. N. Pittet, D. G. Kirchner, M. Steindorfer, D. Kucharski, D. Cerutti-Maori, J. Rosebrock, S. Sommer, L. Leushacke, P. Karrang, R. Kanzler, and H. Krag, "Debris attitude motion measurements and modelling by combining different observation techniques," in *7th European Conference on Space Debris*, Darmstadt, Germany: ESA Space Debris Office, 2017.

[25] E. Linder, J. Silha, T. Schildknecht, and M. Hager, "Extraction of spin periods of space debris from optical light curves," in *Proceedings of 66th International Astronautical Congress*, International Astronautical Federation (IAF), 2015. DOI: 10.7892/boris.73954.

[26] ESA, *ESA ClearSpace-1*, 2019. [Online]. Available: https://bit.ly/3ij9Ede (visited on 09/28/2020).

[27] United Launch Alliance, *Atlas V Launch Services User's Guide*, March. United Launch Alliance, 2010. [Online]. Available: http://www.ulalaunch.com/uploads/docs/AtlasVUsersGuide2010.pdf.

[28] Arianespace, "Ariane 5 User's Manual," Arianespace, Tech. Rep. 5, 2016.

[29] Space Exploration Technologies Corp, "Falcon User' s Guide," Space Exploration Technologies Corp, Tech. Rep. April, 2020.

[30] Arianespace, "Soyuz User's Manual," Arianespace, Tech. Rep. 2, 2012.

[31] A. Zak, *Volga upper stage*, 2016. [Online]. Available: http://www.russianspaceweb.com/volga.html.

[32] Arianespace, "Vega User's Manual," Arianespace, Tech. Rep. 4, 2014.

[33] United Launch Alliance, *Delta IV Launch Services User's Guide*, June. United Launch Alliance, 2013.

[34] K. Yoshida, "Engineering test satellite VII flight experiments for space robot dynamics and control: Theories on laboratory test beds ten years ago, now in orbit," *International Journal of Robotics Research*, vol. 22, no. 5, pp. 321–335, 2003. DOI: 10.1177/0278364903022005003.

[35] K. Yoshida and S. Abiko, "Inertia parameter identification for a free-flying space robot," *AIAA Guidance, Navigation, and Control Conference and Exhibit*, no. August, pp. 1–8, 2002. DOI: 10.2514/6.2002-4568.

[36] P. K. Nguyen and P. C. Hughes, "Teleoperation: From The Space Shuttle To The Space Station," in *Teleoperation and Robotics in Space*, American Institute of Aeronautics and Astronautics, Jan. 1994, pp. 353–410. DOI: 10.2514/5.9781600866333.0353.0410.

[37] S. Vyas, *vyas-shubham/TraceableRobotModels: Release v0.3 of Traceable Robot Models*, Jul. 2020. DOI: 10.5281/ZENODO.3930786.

[38] M. Wilde, S. K. Choon, A. Grompone, and M. Romano, "Equations of motion of free-floating spacecraft-manipulator systems: An Engineer's tutorial," *Frontiers Robotics AI*, vol. 5, no. APR, pp. 1–24, 2018. DOI: 10.3389/frobt.2018.00041.

[39] D. N. Dimitrov and K. Yoshida, "Momentum distribution in a space manipulator for facilitating the post-impact control," *2004 IEEE/RSJ International Conference on Intelligent Robots and Systems (IROS)*, vol. 4, 2004. DOI: 10.1109/iros.2004.1389933.

[40] D. Dimitrov and K. Yoshida, "Utilization of the bias momentum approach for capturing a tumbling satellite," in *2004 IEEE/RSJ International Conference on Intelligent Robots and Systems (IROS) (IEEE Cat. No.04CH37566)*, vol. 4, IEEE, 2004. DOI: 10.1109/IROS.2004.1389931.

[41] KUKA AG, "KUKA robots for heavy payloads from 360kg to 1,000kg. Brochure," Tech. Rep., 2018.

[42] J. Virgili-Llop and M. Romano, "Simultaneous capture and detumble of a resident space object by a free-flying spacecraft-manipulator system," *Frontiers Robotics AI*, vol. 6, no. MAR, 2019. DOI: 10.3389/frobt.2019.00014.